Cloud-radiation interactions and cloud-climate feedbacks from an active-sensor satellite perspective

Grégory Cesana[1,2] and Andrew Ackerman[2], Thibault Vaillant de Guélis[3,4], and David S. Henderson[5]

[1] Columbia University, Center for Climate Systems Research, Earth Institute, New York, NY
[2] NASA Goddard Institute for Space Studies, New York, NY.
[3] Science Systems and Applications, Inc., Hampton, VA 23666, USA
[4] NASA Langley Research Center, Hampton, VA 23681, USA.
[5] Space Science and Engineering Center, University of Wisconsin–Madison, Madison, Wisconsin

Correspondence to: Gregory V. Cesana (gregory.cesana@columbia.edu)

Abstract

Clouds are ubiquitous in the troposphere. Their interactions with radiation may result in either a warming or a cooling of the Earth system and generate diverse climate feedbacks. The vertical structure of the radiative effects of clouds as well as the response of clouds to global warming (i.e., the cloud feedbacks) are inadequately constrained within the diversity of current climate models, which limits our ability to project the magnitude of future warming. In this chapter we show how relatively recent active-sensor spaceborne observations have narrowed constraints on cloud feedbacks. The value added beyond what can be retrieved from passive sensors is only just beginning to be exploited.

1. Introduction

The interactions between cloud particles and radiation modulate the amount of energy that is reflected, emitted, and absorbed by the Earth. Changes in cloud properties (e.g., areal and vertical extent, temperature, emissivity, opacity, and absorptivity profiles) modify their radiative effects, which, in turn, can profoundly affect the radiative balance of the Earth-atmosphere system (Kiehl & Trenberth, 1997; Wielicki et al., 1996) because clouds cover a large part of the troposphere (Cesana & Waliser, 2016; Stubenrauch et al., 2013). For example, liquid clouds are typically more opaque than their frozen counterparts, which corresponds to more reflection of shortwave (SW) radiation and also more absorption and emission of longwave (LW) radiation for a given profile of water content and temperature (e.g., Cesana and Storelvmo, 2017; Rogers and Yau, 1989).

For the past few decades, passive sensor satellites have been monitoring cloud properties (e.g., Rossow & Schiffer, 1999) and the outgoing and incoming radiative fluxes at the top of the atmosphere (e.g., Wielicki et al. 1996) . More recently, active sensors onboard the Cloud–Aerosol Lidar and Infrared Pathfinder Satellite Observations (CALIPSO; Winker et al., 2010) and CloudSat (Stephens et al., 2002) flying in the A-Train Constellation have provided detailed vertical distribution of cloud properties. Combining these new observations with passive sensor information from other A-Train satellites has made it possible to characterize radiative fluxes at a high vertical resolution for different types of clouds (Hang et al., 2019; L'Ecuyer et al., 2019; Matus & L'Ecuyer, 2017) and has improved previous estimates of surface and top-of-atmosphere (TOA) radiative fluxes (Stephens et al., 2012).

To better understand past, present and future climates, we partly rely on Earth system models (ESMs), which are a simplified version of nature and whose utility and plausibility can be evaluated to some extent through rigorous comparison with pertinent observations. Because of their coarse horizontal mesh of O(100 km), climate models by design do not resolve cloud processes on smaller scales, instead relying on parameterizations that represent the expressions of subgrid processes on the gridbox scale. Often times, such oversimplification results in large cloud biases (e.g., Klein et al., 2013; Zhang et al., 2005). With its more detailed vertical information, CloudSat-CALIPSO observations have exposed biases in climate models (e.g., Cesana and Waliser, 2016; Jiang et al., 2012; Nam et al., 2012) beyond the reach of previous satellite observations. However, it is assumed that simulating the current cloud climatology is a necessary but not sufficient condition to build confidence in the ability of the models to reliably project future climate change.

When subjected to "external" forcings, such as anthropogenic changes in atmospheric greenhouse gases, the atmosphere and surface warm at a rate determined not only by the forcing itself, but also by positive and negative feedbacks, defined as changes in the climate system in response to the forcing that respectively amplify and reduce the warming. Of all the feedbacks (i.e., Planck, water vapor, temperature lapse rate, surface albedo), those associated with changes in clouds in both the current and previous Coupled Models Intercomparison Project (CMIP) generations remain the largest source of uncertainty in Earth's equilibrium climate sensitivity (ECS) in ESMs, which is a measure of the warming resulting from a doubling of CO2 levels (Andrews et al., 2012; Bony & Dufresne, 2005; Caldwell et al., 2016; Vial et al., 2013; Zelinka et al., 2016, 2020). Such diverse behavior limits our ability to project the magnitude of future climate change impacts. Being able to simulate cloud properties accurately is therefore critical to narrowing down the uncertainty in cloud feedbacks and their associated spread in models' ECS, and ultimately, improve our confidence in projections of future climate change impacts.

In this article, we focus on recent advances made in monitoring cloud-radiation interactions from active-sensor satellite observations (section 2) and how these observations have been used to estimate and improve our understanding of cloud feedbacks (section 3).

2. Cloud-radiation interactions

Cloud radiative heating rates

Although passive sensor satellites have been monitoring the outgoing and incoming radiative fluxes at TOA for an extended period of time (e.g., Wielicki et al. 1996), vertically resolved profiles of such fluxes have been lacking. L'Ecuyer et al., (2009) first developed a new radiative flux retrieval based on CloudSat measurements and a radiative transfer model. A few years later, this product integrated other A-Train satellite measurements from CALIPSO (Winker et al., 2010) and Moderate Resolution Imaging Spectroradiometer (MODIS, King et al., 2013) to take into account the contribution of thin cirrus and near surface shallow clouds and aerosols (the 2B-FLXHR-LIDAR product, Henderson et al., 2013). In parallel, another combined product was developed by an independent group also based on CloudSat-CALIPSO-MODIS but with the addition of CERES information: the CERES-CALIPSO-CloudSat-MODIS (CCCM, Kato et al., 2011).

Before the active sensor satellite era, the evaluation of the radiative effect of clouds on a global scale was limited to the TOA (e.g., Wang and Su, 2013) and the surface, although with less confidence (e.g., Wild et al, 2015). In addition to providing a more complete view of the radiative fluxes at both the surface and TOA (Stephens et al., 2012), these aforementioned active-sensor observations provide new opportunities to document the radiative heating rate contribution of the clouds at an unprecedented vertical resolution (Haynes et al., 2013) and thereby enable further evaluation of climate models on a global scale (Cesana et al., 2019a). Figure 1 shows zonal profiles of cloud radiative heating rate (RHR) for the A-Train observations, the average of five ESMs and its bias (Cesana et al., 2019a). The simulated clouds produce too little warming in the lowest levels compared to the observations (blue shading in the bottom plot) as opposed to an excess of warming in the high levels, particularly in the tropics. Both of these biases are driven by the infrared component and explained by biases in cloud properties. In the low levels, the cloud amount and cloud-top height is underestimated by the models while in the high levels, the models produce excessive cloud fraction and ice water content compared to the observations (Cesana et al., 2019). The cloud RHR biases highlighted here are likely to cause an amplification of cloud biases in climate models. For example, the excess of warming in the high levels may modify the convection (Li et al., 2016) whereas the lack of warming near the surface may prevent the clouds from lifting up and reinforce the cloud biases (Brient & Bony, 2012).

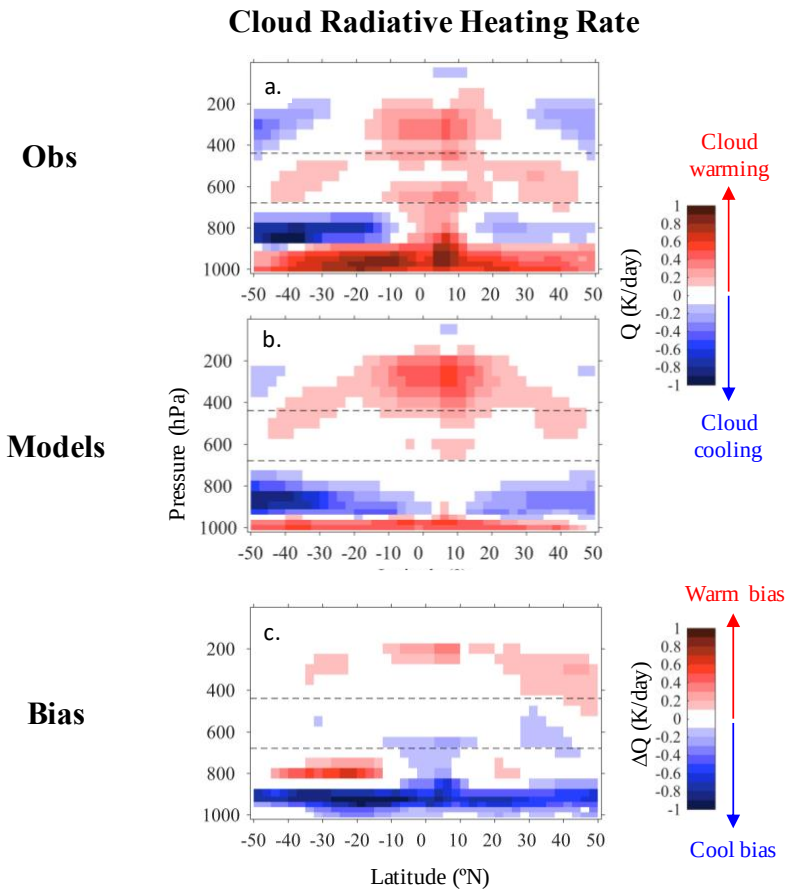

Figure 1: Cloud radiative heating rate biases in climate models. *Zonal profiles (x-axis, latitude [˚]; y-axis, pressure [hPa]) of annual mean total cloud radiative heating rate (K/day) for the A-Train observations (top, 2007-2010 daytime and nighttime, monthly files) for the multimodel mean (middle, 5 models, 1991-2008) and the multimodel mean bias (bottom). Horizontal black dashed lines separate the low- and mid-level clouds (680 hPa), and mid- and high-level clouds (440 hPa). The red and blue shading designate cooling and warming, respectively. To highlight significant model error estimates, only biases larger than the observed maximum uncertainty estimates are shown in the bottom plot. Note that simulated data poleward 50˚ were not requested in this model experiment. Modified from Cesana et al. (2019a).*

Cloud radiative effects as a function of the cloud phase

Combined A-Train observations make it possible to quantify cloud radiative effects not only at the surface, within the atmosphere and at TOA but also as a function of the cloud phase. Cloud phase is of particular interest since liquid and ice clouds generally have very distinct radiative properties. Clouds composed of liquid drops have greater numbers of cloud particles that are smaller in size than their frozen counterparts for a given water content. As a result, their optical depths are larger than that of the ice clouds (Rogers and Yau, 1989), which results in more reflection of solar radiation and also more emission of infrared radiation for a cloud at the same temperature (e.g., Cesana & Storelvmo, 2017).

At middle and high latitudes, when the temperature drops below 0˚C, clouds that contain both supercooled liquid water and ice are referred to as mixed-phase clouds. These clouds are usually topped by a thin supercooled layer with underlying ice crystals that continue to grow below the liquid cloud base where the air is supersaturated with respect to ice (e.g., Fridlind and Ackerman, 2018). Such clouds can be challenging to detect with passive-sensor satellites (e.g.,

Cesana et al., 2016; Stubenrauch et al., 2013) and climate models struggle to accurately represent them (Cesana et al., 2012, 2015; Klein et al., 2009; Komurcu et al., 2014; McIlhattan et al., 2020). While mixed-phase clouds are estimated to only account for 10% of total cloud cover (less than either type of single-phase cloud), their net radiative impact relative to all clouds is estimated to be around 20% (Matus & L'Ecuyer, 2017), based on 2B-FLXHR-LIDAR observations. This product uses lidar and radar signal intensity differences between liquid and ice particles, relying on the fact that the lidar is highly sensitive to small particles (i.e., droplets) while the radar is more sensitive to larger particles (i.e., ice crystals). In addition, mixed-phase clouds also influence atmospheric and even oceanic circulations (Matus & L'Ecuyer, 2017). Thus, assessing their presence and radiative effect in climate models is an important step toward improving climate simulations and how clouds could respond to climate warming, which now may be undertaken using these new active-sensor based observations.

For example, Figure 2 quantifies the TOA cloud radiative fluxes as observed by CERES observations and partitioned by phase as observed by CALIPSO-GOCCP in each grid box. The CALIPSO-GOCCP cloud phase observations (Cesana & Chepfer, 2013) provides 333 m-along-track-resolution near-nadir lidar profiles for 480 m height intervals. Unlike 2B-FLXHR-LIDAR, which uses the different sensitivities of the lidar and radar to small and large particles (typically water droplets and ice crystals,respectively) to determine the cloud phase, CALIPSO-GOCCP utilizes the state of polarization of the lidar beam to separate between liquid and ice clouds, which results in a good agreement with airborne in situ measurements (Cesana et al., 2016). A non-spherical ice crystal changes the polarization state of the lidar return, unlike a spherical liquid droplet. Whether a gridbox is dominated by ice or liquid-containing clouds, which often correspond to mixed-phase clouds at subfreezing temperatures (Silber et al., 2020), is determined by the ratio of ice to ice plus liquid cloud frequencies (above and below one half for ice or liquid dominated clouds, respectively). The results clearly show distinct contribution of the two phase regimes in terms of TOA radiative forcings, with differences up to 60 W/m^2 (Fig. 2, right).

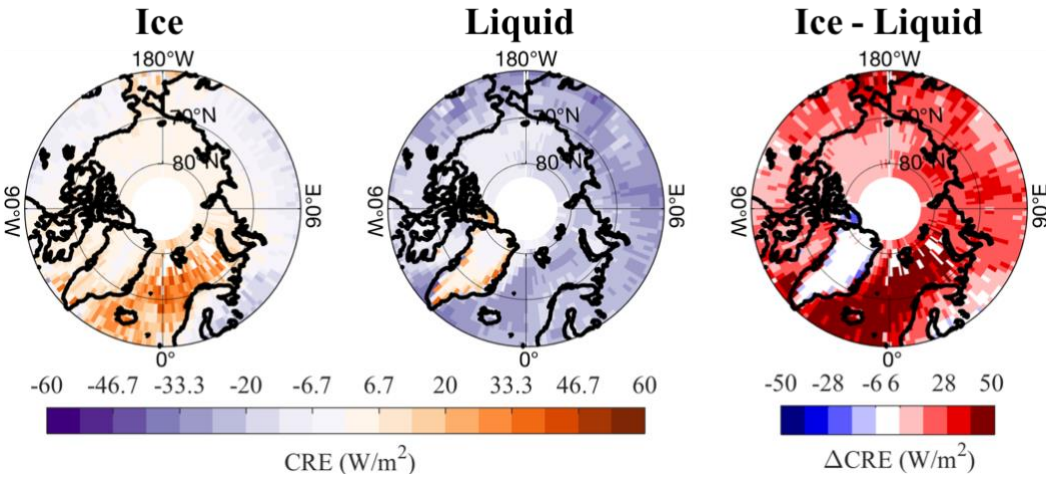

Figure 2: Cloud radiative effect as a function of the phase regime. *Monthly CERES-EBAF (Loeb et al., 2018) averaged net CRE at the TOA for ice-dominated (left column), liquid-dominated gridboxes (middle column) and the difference (right column) based on CALIPSO-GOCCP frequency phase ratio (2007-2016 daytime and nighttime; Cesana et al., 2016).*

Multilayered clouds

Finally, by documenting nearly all vertical levels of the troposphere for every profile, the combined A-Train observations (e.g., 2B-FLXHR-LIDAR) also allow the distinction of radiative contributions from single-layer and multilayered clouds. Using this capability, recent studies (Hang et al., 2019; L'Ecuyer et al., 2019; Matus & L'Ecuyer, 2017) have shown that multilayered clouds, which correspond to multiple non-contiguous cloudy layers in the same profile, are ubiquitous and exert a strong influence on TOA energy balance and atmospheric heating. More specifically, they report that the largest contribution to global CRE at TOA and two third of atmospheric radiative heating is associated with multilayered clouds, which are often misclassified as geometrically-thick mid-level clouds by passive-sensor instruments. This novel result gives raise to the question of the extent to which radiative biases in ESMs are related to poor representation of multilayered cloud systems, a problem that has been suggested as most likely attributable to the use of oversimplified vertical overlap assumptions (Barker, 2009; Cesana & Waliser, 2016; Hogan & Illingworth, 2000).

3. Constraining cloud feedbacks

Different cloud feedbacks

Within the context of global warming, the radiative impact of clouds in response to surface temperature variations, referred to as cloud feedback, remains the largest source of uncertainty in ESMs' climate sensitivity (e.g., Andrews et al., 2012; Caldwell et al., 2016; Zelinka et al., 2020). The cloud feedback can be decomposed into three main components (Fig. 3, middle column) coming mostly from high and low clouds (cloud top above ~ 7 km and below ~ 3 km, respectively). In the CMIP5 models, the first and largest component is the cloud cover feedback, mostly contributed by tropical and midlatitudes low clouds. On average, tropical low clouds are expected to dissipate somewhat, which would result in more incoming solar radiation, reinforcing the surface warming through a positive feedback (with an ensemble mean of + 0.35 W m^{-2} K^{-1}). It is also the most uncertain one with values ranging roughly from -1 W m^{-2} K^{-1} to 2 W m^{-2} K^{-1} (e.g., Klein et al., 2017; Cesana and Del Genio, 2021). The second component is the altitude feedback (+ 0.2 W m^{-2} K^{-1}), which results from changes in altitude while keeping the cloud amount and optical depth fixed. This feedback is positive where high clouds rise higher in response to warming, hampering surface LW cooling. The third is the opacity feedback (- 0.11 W m^{-2} K^{-1}), the only negative feedback out of the three, which is due to an increase in cloud optical depth from ice and mixed-phase clouds turning into liquid clouds with warmer temperatures. As a result, the amount of SW radiation reflected back to space is increased, thereby reducing the initial surface temperature warming (negative feedback).

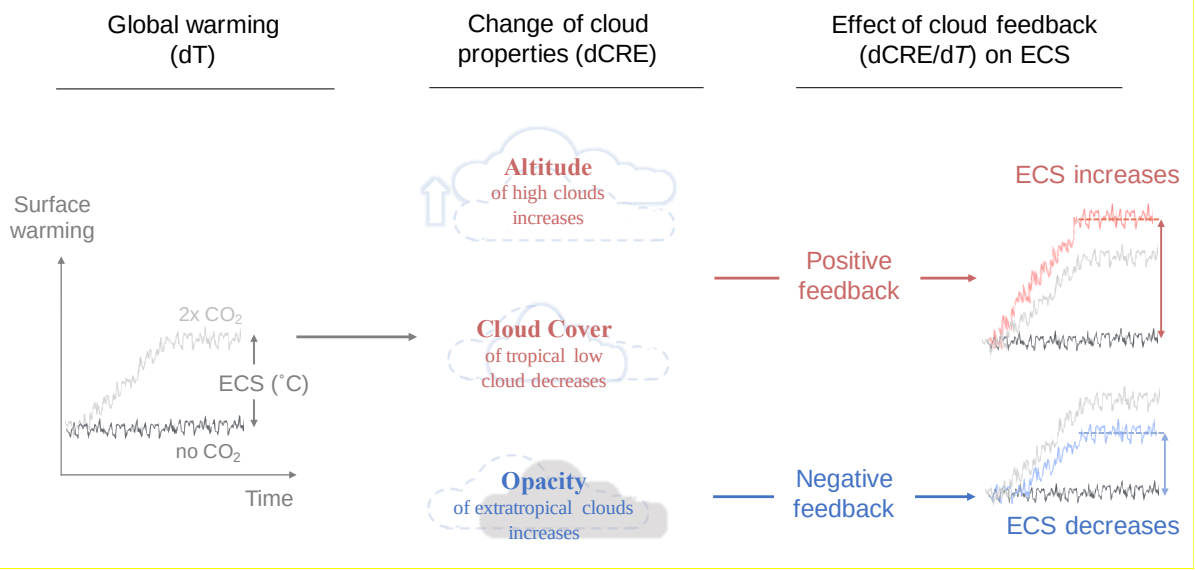

Figure 3: Illustration of the main cloud feedbacks and their impacts on climate sensitivity*. The global mean surface temperature warms in response to an instantaneous doubling of CO_2 concentrations (light gray line, left column) relative to the pre-industrial atmosphere (dark grey line). At equilibrium, the temperature difference between the two curves defines the equilibrium climate sensitivity (ECS). That anthropogenic-induced warming alters cloud properties (middle column): high clouds rising higher, tropical low clouds dissipating and extratropical clouds becoming optically thicker. As a consequence, their cloud radiative effects also change and feeds back on the surface temperature by either enhancing the initial warming, a positive feedback (altitude and cloud cover feedbacks), or weakening it, a negative feedback (opacity feedback). Ultimately, the positive and negative feedbacks contribute to increasing and decreasing the ECS, respectively (right column).*

Interannual cloud feedbacks

Capturing the mechanisms that govern the change of clouds in response to a surface warming is therefore necessary – but not sufficient – to reliably predict future climate. As a result, numerous studies have been devoted to evaluating the sensitivity of clouds to surface temperature in climate models against observations (e.g.; Cesana et al., 2019c; McCoy et al., 2017; Myers and Norris, 2016; Qu et al., 2015). Most of these studies focus on the positive low-cloud feedbacks since multimodel spread of tropical low-cloud feedbacks dominates the uncertainty in model estimates of ECS (Andrews et al., 2012; Bony & Dufresne, 2005; Caldwell et al., 2016; Vial et al., 2013).

For example, the interannual variation of low clouds and their radiative effects (i.e., interannual low-cloud feedbacks) drive the low-cloud feedbacks through their physical relationships with sea surface temperature (SST) and estimated inversion strength (EIS; Qu et al., 2014), the two main cloud-controlling factors (CCF), which appear to be time-scale invariant (i.e., to hold in the future climate; Klein and Hall, 2015; Zhou et al., 2015a). These interannual cloud feedbacks can be derived from satellite observations in both the SW and the LW and used to evaluate models (e.g., Fig. 4e; Cesana et al., 2019a) and to constrain their low-cloud feedbacks (e.g., Cesana et al., 2019a ; Myers and Norris, 2016).

A series of studies focused on the interannual variability of low clouds (described above) have shown that the low-cloud amount as observed from space substantially decreases in response to

a surface warming. Such a decrease of low clouds generates a weakening of their negative SW cloud radiative effect (CRE) at TOA, which is defined as the difference between clear- and all-sky TOA SW fluxes. As a consequence, less SW radiation is reflected back to space and low clouds contribute to further warming the system through a positive feedback. Figure 4 shows the tropical low-cloud fraction (LCF) in subsidence regimes (ω_{500} > 10 hPa/d) from various active- and passive-sensor satellite products. Although the LCF amplitude (Fig. 4a) can vary substantially from one product to another (mainly due to different detection sensitivities, cloud definitions and retrieval method), its interannual variability with respect to SST and EIS (Fig. 4b and 4c) is robustly depicted by all products. In agreement with previous studies (Cesana and Del Genio, 2021; Cesana et al., 2019c; Myers and Norris, 2016; Zhou et al., 2015a), the LCF largely decreases with increasing SST (Fig. 4b; - 2.4 %/K on average) whereas it slightly increases with increasing EIS (Fig. 4c; 1 %/K on average). On the one hand, an increasing SST corresponds to a stronger vertical gradient of specific humidity, which contributes to drying of the planetary boundary layer (PBL), therefore reducing the cloud amount. On the other hand, a stronger inversion leads to less mixing of the PBL with the free troposphere, which reduces the PBL height and favors cloud formation and persistence. In this example, the added value of active-sensor observations is not obvious, but Cesana et al. (2019c) showed that models with a similar low-cloud interannual variability (e.g., ∂LCF/∂SST) could be further constrained with the interannual variability of global cloud profiles using CALIPSO-GOCCP and the lidar simulator. Much uncertainty remains on how controlling factors affect different low-cloud types, but here again, active-sensor satellite can help to advance understanding of the mechanisms at play.

Sc and shallow Cu clouds

Low clouds may be separated into two main categories: stratocumulus (Sc, including stratus clouds) and shallow cumulus (Cu). Sc typically produce nearly overcast conditions off the west coasts of continents, where PBL depth is limited by large-scale subsidence and PBL mixing is primarily driven by cloud-top LW cooling, and they reflect much more SW radiation than the underlying sea surface. Downwind in the extensive open ocean trade-wind regions further west, the Sc decks transition to more scattered Cu cloud fields sustainted by convective updrafts emerging from the loosely coupled surface layer, with a weaker radiative effect. Since the convection in these low clouds is driven by different processes, they are not expected to exhibit the same feedback. Satellite observations hint that low clouds in regions dominated by Sc show somewhat different interannual variations than in regions dominated by shallow Cu (Cesana, et al., 2019c). In addition, idealized large-eddy simulation (LES) studies shows that feedbacks from Sc and Cu clouds can be substantially different (Bretherton, 2015). This has been confirmed in a recent satellite-based study over the whole tropics, the Sc cloud produce a much larger positive feedback than the Cu, regardless of the future SST and EIS trends (Cesana and Del Genio, 2021). Yet understanding of the underlying reasons remains incomplete, particularly for trade-wind Cu , which may even produce negative feedbacks in response to surface warming in LES studies (Narenpitak & Bretherton, 2019).

Without having access to the vertical structure of the low clouds (i.e., with passive sensor measurements), it is particularly challenging to tell Sc and Cu types apart. This caveat has been alleviated with the use of active-sensor satellites (Cesana et al., 2019b). Figure 4 also shows low-

cloud fractions and interannual variations of Sc- and shallow Cu-dominated regimes from some active- and passive-sensor satellite observations (Table 1). The Sc and Cu regimes are determined using three different methods described into detail by Cesana et al. (2019). Sc and Cu clouds have been commonly distinguished by joint distributions of cloud-top pressure and optical thickness in passive-sensor observations (Rossow & Schiffer, 1999), although this method has been shown to misclassify Sc and Cu clouds that have moderate optical thickness (Pincus et al., 2012) and to mix different cloud types together (Mace & Wrenn, 2013). The newer passive-sensor clustering approaches, such as the ISCCP weather states (Tselioudis et al., 2013) and MODIS cloud regimes (Oreopoulos et al., 2014), do not discriminate cloud types but rather regimes of prevalent cloud types. As such, they cannot be compared directly to Sc and Cu cloud types. Finally, the new CASCCAD-based active-sensor observations (both CALIPSO-CASCCAD and CloudSat-CALIPSO-CASCCAD products) separates Sc from shallow Cu clouds at the orbital level (i.e., for every profile) based on their morphology using additional information on cloud height and vertical and horizontal cloud fraction variation, improving Sc-Cu classification compared to previous techniques using passive-sensor satellite observations (Cesana et al., 2019b).

Table 1: Description of the datasets that are used in Fig. 4.

Product	CAL-CASCCAD	CC-CASCCAD	ISCCP-H1	MODIS-C5-retrieval	MISR V6	ISCCP-D1 Weather State	MODIS-C6 Cloud Regime
Satellite	CALIPSO	CloudSat-CALIPSO	Multiple weather and polar-orbiting satellites	Aqua/Terra	Terra	Multiple weather and polar-orbiting satellites	Aqua/Terra
Active/passive sensor	active	active	passive	passive	passive	passive	passive
Instrument	Lidar (532 nm)	Lidar (532 nm) and radar (94 GHz)	Multispectral imagers	Multispectral imagers	Multispectral + multiangle imagers	Multispectral imagers	Multispectral imagers
Sc-Cu discrimination	Cloud morphology (cloud height, horizontal cloud fraction and vertical cloud fraction variability)	Cloud morphology (cloud height, horizontal cloud fraction and vertical cloud fraction variability)	Cloud-top pressure and optical depth	Cloud-top pressure and optical depth	Cloud-top height and optical depth	clustering (weather state)	clustering (cloud regime)
Time period	2007-2016	2007-2010	2007-2016	2007-2015	2007-2016	1984-2007	2003-2014
Reference	Cesana et al. (2019b)	Cesana et al. (2019b)	Rossow and Schiffer (1999)	Pincus et al. (2015)	Marchand et al. (2010)	Tselioudis et al. (2013)	Oreopoulos et al. (2014)

Consistent with previous literature (Bretherton et al., 2015; Cesana and Del Genio, 2021; Cesana et al., 2019c), the Sc and shallow Cu responses to SST and EIS are substantially different regardless of the satellite observations considered. The Sc cloud fraction largely decreases and increases with increasing SST and EIS, respectively (Fig. 4e and f), while shallow Cu cloud fraction barely varies with SST and may either decrease (CASCCAD and ISCCP weather state observations) or remain almost invariant (other passive-sensor observations) with increasing EIS (Fig. 4h and i). Although all considered satellite observations more or less agree on the sign and amplitude of the low cloud interannual variations (Fig. 4b and c), only active-sensor CASCCAD observations capture their variability with respect to EIS when decomposed into Sc and Cu cloud regimes. We note that the agreement between active- and passive-sensor observations is far better when Sc and Cu cloud regimes are determined using CALIPSO-CASCCAD for overlapping periods (not shown). Such results – made possible by active-sensor satellite observations – provide a robust observational target for model evaluation and pave the way for new studies exploring the cloud processes behind the distinct behaviors of Sc and shallow Cu clouds in response to SST and EIS forcings.

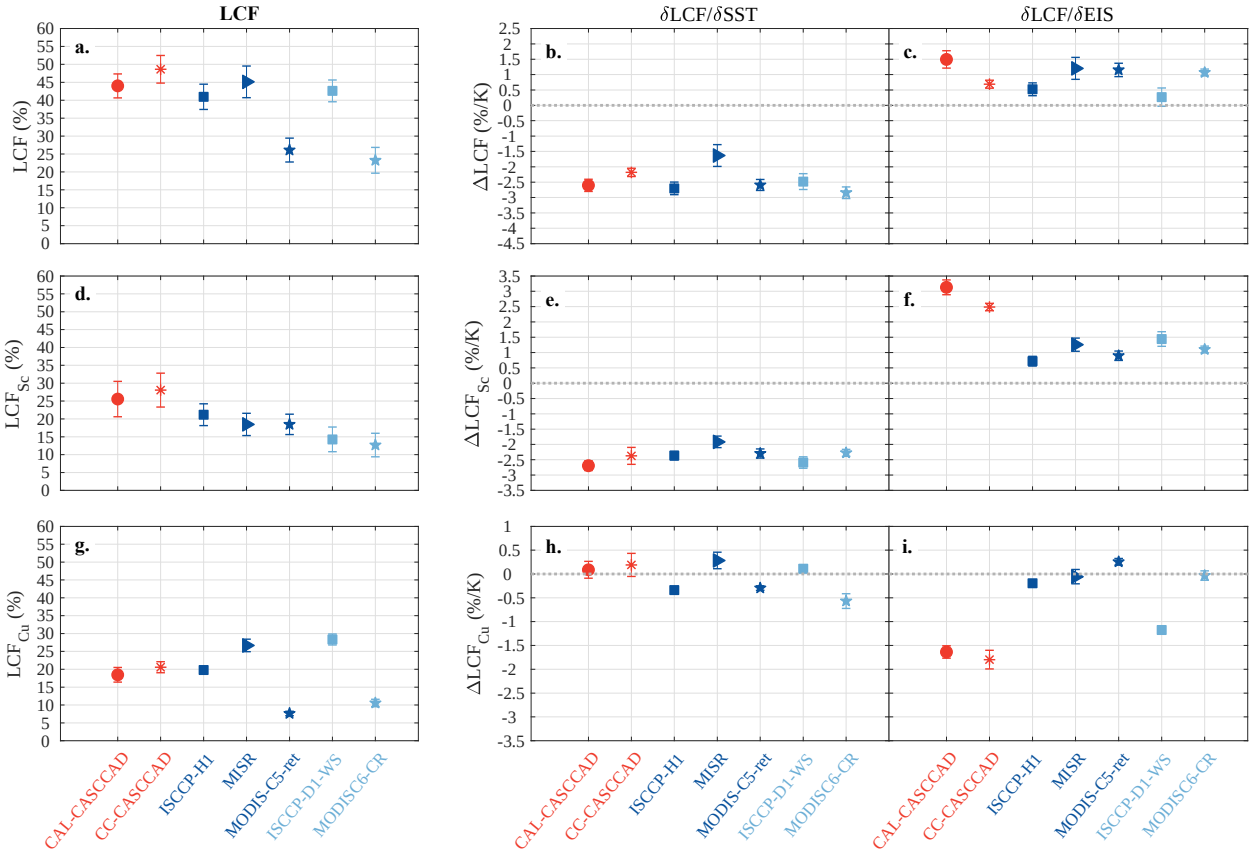

Figure 4: Low-cloud sensitivities of Sc- and shallow Cu-dominated to cloud-controlling factors. *Observed low-cloud fraction (%) in subsidence regimes over the tropical oceans (ω500 > 10 hPa/day) for different satellite datasets (the active-sensor products in red and the passive-sensor products in blue shading) for all low clouds, for stratocumulus dominated regions and for shallow cumulus dominated regions (left column, from top to bottom, respectively). Observed interannual low-cloud change per K of SST warming with EIS held constant (∂LCC/∂SST, % K^{-1}; middle column) and per K of EIS increase with SST held constant (∂LCC/∂EIS, % K^{-1}; right column) for the same satellite products and using six observational and reanalysis products for the SST and EIS datasets. The uncertainty bars correspond to the interannual mean variability for the cloud fractions (left column), and the 10-90% confidence interval using the three SST and EIS datasets for the partial derivatives (middle and right columns). The method to compute these partial derivatives is described in Cesana et al. (2019a). See the text for the different methods used to discriminate*

Sc and Cu clouds in each product. In order of appearance in the plots, the satellite dataset used are (see also Table 1): CALIPSO-CASCCAD (2007-2016) and CloudSat-CALIPSO-CASCCAD (2007-2010; Cesana et al., 2019b), ISCCP-H1 (2007-2016; Rossow and Schiffer, 1999), MISR-V6 (2007-2016; Marchand et al., 2010), MODIS-C5 (2007-2015; Pincus et al., 2012), ISCCP-D1 weather state (1984-2007; Tselioudis et al., 2013) and MODIS-C6 cloud regimes (2003-2014; Oreopoulos et al., 2014)*. The dark and light blue shadings distinguish two different methods of Sc and Cu discrimination used in passive-sensor observations (see Table 1 and text for more details).*

Inferring low-cloud feedbacks from observations

Assuming that the relationships (i.e., the partial derivatives such as Fig. 4, middle and right columns) between low clouds and their controlling factors remain effectively identical in a future climate, they may be used to estimate the future change of low clouds in combination with the change in each controlling factors derived from multimodel climate projections (i.e., the difference between future climate and controle climate, e.g., Klein et al., 2017; Myers and Norris, 2016). As a result, one can infer an observationally based estimate of the low-cloud change by using the observed partial derivatives of each controlling factor multiplied by their change obtained from future climate projections of multiple models as in Myers and Norris (2016, their Fig. 2). Then, the observationally inferred future cloud feedbacks can be found by simply changing the sign of the observationally inferred low-cloud change since the two quantities are almost perfectly negatively correlated (Cesana et al., 2019a; Klein et al., 2017). Using this method and multiple estimates of partial derivatives with respect to SST and EIS from past studies, Klein et al. (2017) found that the tropical global mean cloud feedback is 0.25 ± 0.18 W m^{-2} K^{-1} (90% confidence interval), consistent with previous evidence suggesting that the tropical low-cloud net feedback is positive. However, Cesana and Del Genio (2021) show that because Sc and shallow Cu clouds have different responses to controlling factors (see Fig. 4) and cover distinct geographic areas (Cesana et al., 2019a), their inferred feedback must be computed separately and added up to estimate the inferred low-cloud feedback. By doing so, the inferred low-cloud feedback and its uncertainty estimates are two times smaller than that computed without separating Sc and shallow Cu contributions as in past studies using passive-sensor observations. Using active-sensor satellite observations, we can now reliably determine the separate sensitivities of Sc and Cu clouds to their controlling factors (Fig. 4, middle and bottom rows) and subsequently infer more accurate, less uncertain low-cloud feedbacks (Cesana and Del Genio, 2021) than previous estimates (e.g., Klein et al., 2017).

Extratropical (opacity) cloud feedbacks

Low clouds also produce substantial feedbacks in the extra-tropics, which can be either positive or negative, in response to changes in their amount and microphysical properties (Tsushima et al., 2006; Zelinka et al., 2016, 2020). Most of the increase in ECS between CMIP5 and CMIP6 models has been linked to extratropical low-cloud feedbacks (Zelinka et al., 2020), which is mainly determined by its SW component. The macrophysical processes leading to a change in cloud amount should be the same as those in the tropics, but the mechanisms involved in the change in microphysical properties remain unclear. Past studies showed that the extratropical cloud feedback greatly depends on the sensitivity of cloud phase and cloud opacity to climate warming (Ceppi et al., 2016; Terai et al., 2016) but these feedbacks remain largely unconstrained in the current generation of ESMs (Zelinka et al., 2020). In a warmer climate, more liquid water would form at the expense of ice in such clouds, thereby leading to a larger optical depth and a longer lifecycle (e.g., Cesana & Storelvmo, 2017). As a result, the amount of solar

radiation reflected back to space would be increased, weakening the surface warming (a negative feedback), described in the literature as "optical depth feedback". For the foregoing reasons, documenting separately liquid and ice clouds globally and over the polar regions appears essential to better constraining the optical depth feedback, but doing so from passive-sensor satellite observations is particularly challenging (Baum et al., 2012; Cesana et al., 2016). CloudSat-CALIPSO observations offer unique advantages over passive-sensor satellites by providing the vertical structure of clouds over highly reflective surfaces and by discriminating liquid- and ice-dominated clouds, all of which has led to substantial discoveries on extratropical clouds (Bodas-Salcedo et al., 2016; Kay et al., 2016; Kay & Gettelman, 2009).

Previous attempts to better understand the cloud optical depth feedback using CALIPSO observation as a constraint on the supercooled liquid fraction in the present-day climate confirmed that the strength of the cloud optical depth feedback is tightly connected to the cloud phase response to climate warming (Tan et al., 2016). However, although such constraint on present-day climate in ESMs is arguably necessary, it is not sufficient to guarantee a reliable optical depth feedback in ESM simulations of future climate. Therefore, more work is needed to complement traditional analyses of feedbacks by further breaking down the feedbacks into low cloud regimes and directly evaluating their responses to climate warming through a process-level approach using global-scale satellite observations and reanalysis data. This could be done using the value-added set of CALIPSO observations that discriminate between Sc and shallow Cu clouds, liquid, ice and mixed-phase clouds and also documents their opacities (Cesana, Del Genio, & Chepfer, 2019; Cesana & Chepfer, 2013; Guzman et al., 2017).

High-level cloud feedbacks

With global warming, high-level cloud tops are expected to rise, according to climate models (e.g., Ceppi et al., 2017; Cesana et al., 2017). Because this altitude increase is accompanied by warming of the troposphere, the outgoing LW emission from high-level clouds is expected to hold steady while the LW surface emission increases from warming of the surface (Hartmann and Larson, 2002), and the combined effect is a positive feedback that further warms the surface (Zelinka et al., 2016; Zelinka and Hartmann, 2010). Although it is possible to detect observational evidence of cloud-top pressure change with passive-sensor observations (Norris et al., 2016), doing so requires a long record (25 years), complex data processing to minimize biases and artifacts, and, unfortunately, trends cannot be quantified. In contrast, for a similar record length, cloud-top height information derived from active-sensor satellite observations may be used to precisely estimate such a trend (Chepfer et al., 2014; Takahashi et al., 2019). Moreover, active-sensor satellite observations allow for analysis of the interannual variability of cloud profiles, revealing the altitudes at which cloud fraction changes occur (Li et al., 2012; Saint-Lu et al., 2020) and possibly providing estimates of interannual cloud feedbacks. For example, Zhou et al. (2014) used CALIPSO observations to derive a short-term global net feedback from cirrus clouds, which had been lacking for want of adequate cirrus observations from passive-sensor satellites, and show that this feedback is most likely positive and contributes substantially to total cloud feedback globally.

Another CALIPSO-based study analyzed how changes in cloud properties could affect cloud feedbacks in the LW (mostly driven by non-low clouds, altitude > 3 km; e.g., Zelinka et al., 2016) using a novel technique (Vaillant de Guélis et al., 2018). They characterize LW CRE over oceans using five parameters: cloud altitude (Z_T in Fig. 5) and cover (C in Fig. 5) from opaque and thin clouds separately as well as emissivity (ε in Fig. 5) of thin clouds, where opaque clouds are diagnosed when no surface echo is detected (CALIPSO-GOCCP OPAQ, Guzman et al., 2017). This lidar-based method uniquely turns a lidar's limitation – its attenuation for optical thickness greater than 3 – into a strength, by separating these contributions to present-day (short term) LW cloud feedbacks. Such a separation can also be derived from climate models via a lidar simulator, allowing comparison with observed interannual feedbacks and long-term feedbacks from climate simulations. By doing so over oceans only, Vaillant de Guélis et al. (2018) find that the CALIPSO-derived cloud altitude feedback is positive and dominates the present-day LW cloud feedback in a climate model, consistent with results using long-term LW cloud feedback in ESMs. However, in the observations, its contribution to the present-day LW feedback is smaller than that from changes in the opaque cloud fraction. Their results suggest that LW positive cloud feedback could be overestimated in climate model projections.

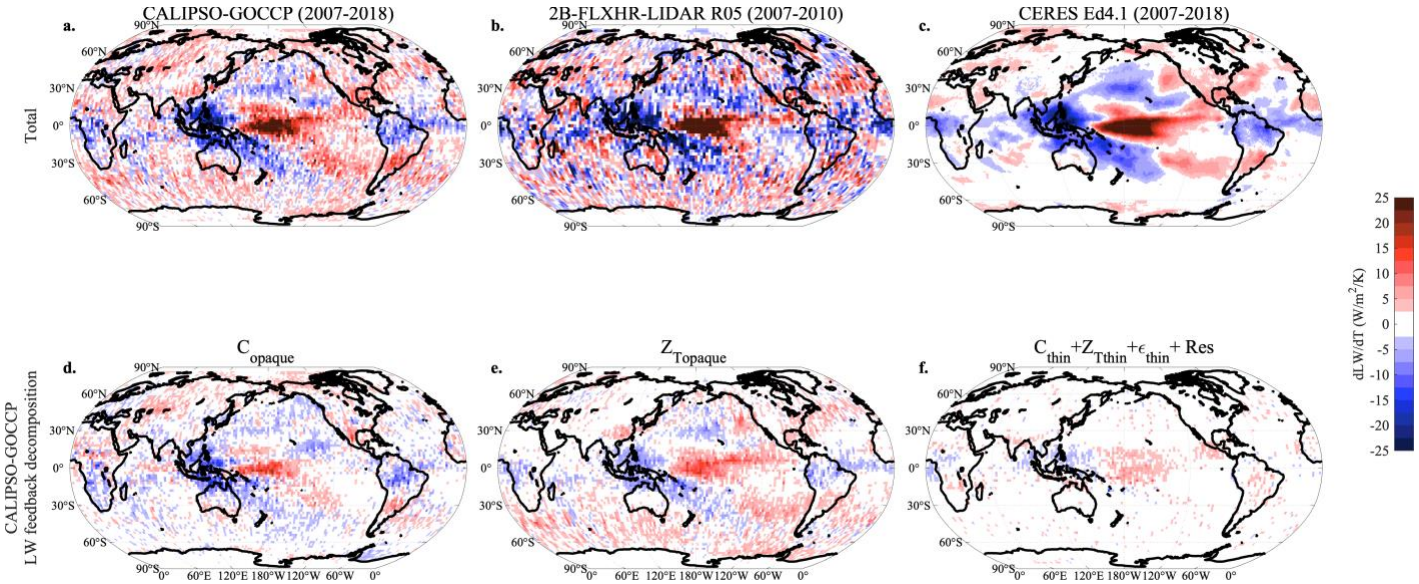

Figure 5: Short-term LW cloud feedback for (a) CALIPSO-GOCCP OPAQ (2007-2018; version 3.1.2), (b) 2B-FLXHR-LIDAR (2007-2010; R05) and (c) CERES (2007-2018; version Ed4.1). Contributions from (d) opaque cloud cover, (e) opaque cloud altitude and (f) thin cloud cover, altitude, emissivity and the residual, all derived from CALIPSO-GOCCP OPAQ. The sum of (d-e-f) panels is equal to (a). Note that changes in opaque cloud cover and altitude are the main contributors to LW cloud feedback.

Following Vaillant de Guélis et al. (2018), we use the CALIPSO-GOCCP observational dataset to derive LW CRE over both oceans and continents and for a longer record. The top panels of Figure 5 show the short-term LW cloud feedbacks from CALIPSO-GOCCP, CloudSat-CALIPSO 2B-FLXHR-LIDAR and CERES observations (top row), and the lower panels its respective decomposition as a function of the five aforementioned cloud properties for CALIPSO-GOCCP. To estimate the LW cloud feedback, we regress monthly anomalies of deseasonalized LW CRE against monthly anomalies of deseasonalized global mean surface temperatures using three different surface temperature datasets (Berkeley Earth Surface Temperature project, Rohde and Hausfather, 2020; GISTEMP v4, Lenssen et al., 2019; HadCRUT 4.6.0.0; Morice et al., 2012).

Although very similar in terms of pattern, the active-sensor based cloud feedbacks are more positive at mid-latitudes, particularly over the Southern Ocean and over continents where the detection of mixed-phase clouds and high-level clouds is challenging for passive-sensor instruments. Even though we use observations over oceans and continents and derive the short-term cloud feedback from interannual instead of seasonal variations as in Vaillant de Guélis et al. (2018), we also find that the main contributors to LW cloud feedback are changes in opaque cloud cover and altitude while the other components only modestly contribute. Such results provide additional information on short-term LW CRE and cloud feedback beyond previous passive-sensor based analysis (e.g., Dessler, 2010; Loeb et al., 2020) owing to the lidar's capabilities, determining cloud-top heights more accurately than passive sensors and detecting optically thin clouds and broken clouds that are often undetected by passive-sensor instruments (e.g., Stubenrauch et al., 2013) despite being radiatively active in the LW.

Radiative kernel-based cloud feedbacks

Radiative kernels quantify the radiative response of the system to small perturbations in a set of climate variables such as the temperature, water vapor and albedo. The radiative kernel approach is often used to compute cloud feedbacks in climate models (Soden et al., 2008; Zelinka et al., 2016, 2020) rather than in observations because cloud information is required at a high vertical resolution. Kramer et al. (2019) took advantage of the CloudSat-CALIPSO ability to compile cloud profiles as well as radiative fluxes to observationally derive radiative kernel-based cloud feedbacks in both the LW and SW, at the surface and TOA, which is a first to our knowledge. Although there are uncertainties related to sampling spatially and within the diurnal cycle, as well as from reliance on reanalysis, this study hold promise for future model evaluation and improved understanding of cloud feedback processes.

4. Summary

Cloud-radiation interactions may result in either a warming or a cooling of the Earth system, generating changes in the large-scale circulation, vertical motions and water cycle. So-called external forcings produce variations of the climate system temperature that modify cloud-radiation interactions by amplifying or reducing temperature changes induced by external forcings, which are called cloud feedbacks. These cloud-radiation interactions, in particular the radiative heating rate profiles of clouds as well as the cloud feedbacks, remain largely unconstrained in climate models, which cause a large spread in the multimodel climate sensitivity. Such diverse behavior limits our ability to project the magnitude of future climate change impacts.

Here we show that the relatively recent active-sensor spaceborne observations have improved our understanding of cloud-radiation interactions (L'Ecuyer et al., 2015; Stephens et al., 2012) by giving us access to the radiative heating rate profiles (Cesana et al., 2019c; Henderson et al., 2013; L'Ecuyer et al., 2009). It also paved the way to new possibilities such as documenting the atmospheric radiative heating and radiative effects of cloud as a function of the

cloud properties. For example, the unique ability of CloudSat-CALIPSO observations to distinguish single and multilayered clouds has revealed the dominant impact of multilayered clouds (Hang et al., 2019; L'Ecuyer et al., 2019; Matus & L'Ecuyer, 2017). Furthermore, these new observations have been used to assess cloud radiative heating rates in climate models for the first time (Cesana et al., 2019c), and will be most likely further used to provide guidance for their future development.

Additionally, we show that active-sensor spaceborne observations improves the discrimination of different cloud types compared to passive-sensor satellite observations (e.g., Sc vs. shallow Cu, liquid vs. ice, opaque vs. thin) and allow us to refine understanding of the response of clouds to environmental factors, which can be further used to infer cloud feedbacks with significantly less uncertainty (Cesana and Del Genio, 2021) or to further decompose contributions of cloud properties to short-term cloud feedbacks (e.g., Fig. 5; Vaillant de Guélis et al., 2018). These new active-sensor based estimates therefore provide novel constraints on ESM short-term and long-term cloud feedbacks (e.g., Cesana and Del Genio, 2021; Vaillant de Guélis et al., 2018), which have remained the main contributor to the spread in models' climate sensitivity.

In the future, new satellite missions (e.g., Aerosol, Cloud, Convection and Precipitation [ACCP]; Earth Clouds, Aerosols and Radiation Explorer [EarthCARE]) will address part of CloudSat-CALIPSO limitations by improving cloud and aerosol detection, particularly close to the surface, with a more sensitive cloud radar and a High Spectral Resolution Lidar (HSRL) and additional instruments (e.g., multi-angle polarimeter; Knobelspiesse et al., 2020). Moreover, these missions will provide additional useful information (microphysics, wind speed, diurnal cycle). We argue that existing CloudSat-CALIPSO observations, combined with those from future missions, when available, should be used at a process level to improve our understanding of cloud-radiation interactions and cloud feedbacks and therefore better quantify the impact of clouds on climate sensitivity.

Acknowledgments

GC and AA were supported by a CloudSat-CALIPSO RTOP at the NASA Goddard Institute for Space Studies. GC would like to thank NASA and CNES for giving access to CALIPSO and CloudSat observations, and Climserv for giving access to CALIPSO-GOCCP observations and for providing computing resources.

References

Andrews, T., Gregory, J. M., Webb, M. J., & Taylor, K. E. (2012). Forcing, feedbacks and climate sensitivity in CMIP5 coupled atmosphere-ocean climate models. *Geophysical Research Letters*, *39*(9), 1–7. https://doi.org/10.1029/2012GL051607

Barker, H. W. (2009). Overlap of fractional cloud for radiation calculations in GCMs: A global analysis using CloudSat and CALIPSO data. *Journal of Geophysical Research Atmospheres*,

114(8), 1–15. https://doi.org/10.1029/2007JD009677

Baum, B. A., Menzel, W. P., Frey, R. A., Tobin, D. C., Holz, R. E., Ackerman, S. A., et al. (2012). MODIS cloud-top property refinements for collection 6. *Journal of Applied Meteorology and Climatology*, *51*(6), 1145–1163. https://doi.org/10.1175/JAMC-D-11-0203.1

Bodas-Salcedo, A., Hill, P. G., Furtado, K., Williams, K. D., Field, P. R., Manners, J. C., et al. (2016). Large contribution of supercooled liquid clouds to the solar radiation budget of the Southern Ocean. *Journal of Climate*, *29*(11), 4213–4228. https://doi.org/10.1175/JCLI-D-15-0564.1

Bony, S., & Dufresne, J. L. (2005). Marine boundary layer clouds at the heart of tropical cloud feedback uncertainties in climate models. *Geophysical Research Letters*, *32*(20), L20806. https://doi.org/10.1029/2005GL023851

Bretherton, C. S. (2015). Insights into low-latitude cloud feedbacks from high-resolution models. *Philosophical Transactions of the Royal Society A: Mathematical, Physical and Engineering Sciences*, *373*(2054). https://doi.org/10.1098/rsta.2014.0415

Brient, F., & Bony, S. (2012). How may low-cloud radiative properties simulated in the current climate influence low-cloud feedbacks under global warming? *Geophysical Research Letters*, *39*(20), 1–6. https://doi.org/10.1029/2012GL053265

Caldwell, P. M., Zelinka, M. D., Taylor, K. E., & Marvel, K. (2016). Quantifying the sources of intermodel spread in equilibrium climate sensitivity. *Journal of Climate*, *29*(2), 513–524. https://doi.org/10.1175/JCLI-D-15-0352.1

Ceppi, P., Hartmann, D. L., & Webb, M. J. (2016). Mechanisms of the negative shortwave cloud feedback in middle to high latitudes. *Journal of Climate*, *29*(1), 139–157. https://doi.org/10.1175/JCLI-D-15-0327.1

Cesana, G., & Waliser, D. E. (2016). Characterizing and understanding systematic biases in the vertical structure of clouds in CMIP5/CFMIP2 models. *Geophysical Research Letters*, *43*(19), 10,538-10,546. https://doi.org/10.1002/2016GL070515

Cesana, G., Kay, J. E., Chepfer, H., English, J. M., & de Boer, G. (2012). Ubiquitous low-level liquid-containing Arctic clouds: New observations and climate model constraints from CALIPSO-GOCCP. *Geophysical Research Letters*, *39*(20), 1–6. https://doi.org/10.1029/2012GL053385

Cesana, G., Waliser, D. E., Jiang, X., & Li, J. L. F. (2015). Multimodel evaluation of cloud phase transition using satellite and reanalysis data. *Journal of Geophysical Research*, *120*(15), 7871–7892. https://doi.org/10.1002/2014JD022932

Cesana, G., Chepfer, H., Winker, D., Getzewich, B., Cai, X., Jourdan, O., et al. (2016). Using in situ airborne measurements to evaluate three cloud phase products derived from CALIPSO. *Journal of Geophysical Research*, *121*(10), 5788–5808. https://doi.org/10.1002/2015JD024334

Cesana, G., Waliser, D. E., Henderson, D., L'Ecuyer, T. S., Jiang, X., & Li, J.-L. F. (2019). The Vertical Structure of Radiative Heating Rates: A Multimodel Evaluation Using A-Train Satellite Observations. *Journal of Climate*, *32*(5), 1573–1590. https://doi.org/10.1175/JCLI-D-17-0136.1

Cesana, Gregory, & Storelvmo, T. (2017). Improving climate projections by understanding how cloud phase affects radiation. *Journal of Geophysical Research*, *122*(8), 4594–4599. https://doi.org/10.1002/2017JD026927

Cesana, Grégory, & Chepfer, H. (2013). Evaluation of the cloud thermodynamic phase in a climate model using CALIPSO-GOCCP. *Journal of Geophysical Research: Atmospheres*, *118*(14), 7922–7937. https://doi.org/10.1002/jgrd.50376

Cesana, Grégory, Del Genio, A. D., Ackerman, A. S., Kelley, M., Elsaesser, G., Fridlind, A. M., et al. (2019). Evaluating models' response of tropical low clouds to SST forcings using CALIPSO observations. *Atmospheric Chemistry and Physics*, *19*(5), 2813–2832. https://doi.org/10.5194/acp-19-2813-2019

Cesana, Grégory, Del Genio, A. D., & Chepfer, H. (2019). The Cumulus And Stratocumulus CloudSat-CALIPSO Dataset (CASCCAD). *Earth System Science Data Discussions*, *2667637*(November), 1–33. https://doi.org/10.5194/essd-2019-73

Dessler, A. E. (2010). A Determination of the Cloud Feedback from Climate Variations over the Past Decade. *Science*, *330*(6010), 1523–1527. https://doi.org/10.1126/science.1192546

Fridlind, A. M., & Ackerman, A. S. (2018). *Simulations of Arctic Mixed-Phase Boundary Layer Clouds: Advances in Understanding and Outstanding Questions*. *Mixed-Phase Clouds: Observations and Modeling*. Elsevier Inc. https://doi.org/10.1016/B978-0-12-810549-8.00007-6

Guzman, R., Chepfer, H., Noel, V., de Guélis, T. V., Kay, J. E., Raberanto, P., et al. (2017). Direct atmosphere opacity observations from CALIPSO provide new constraints on cloud-radiation interactions. *Journal of Geophysical Research*, *122*(2), 1066–1085. https://doi.org/10.1002/2016JD025946

Hang, Y., L'Ecuyer, T. S., Henderson, D. S., Matus, A. V., & Wang, Z. (2019). Reassessing the effect of cloud type on earth's energy balance in the age of active spaceborne observations. Part II: Atmospheric heating. *Journal of Climate*, *32*(19), 6219–6236. https://doi.org/10.1175/JCLI-D-18-0754.1

Haynes, J. M., Vonder Haar, T. H., L'Ecuyer, T., & Henderson, D. (2013). Radiative heating characteristics of Earth's cloudy atmosphere from vertically resolved active sensors. *Geophysical Research Letters*, *40*(3), 624–630. https://doi.org/10.1002/grl.50145

Henderson, D. S., L'ecuyer, T., Stephens, G., Partain, P., & Sekiguchi, M. (2013). A multisensor perspective on the radiative impacts of clouds and aerosols. *Journal of Applied Meteorology and Climatology*, *52*(4), 853–871. https://doi.org/10.1175/JAMC-D-12-025.1

Hogan, R. J., & Illingworth, A. J. (2000). Deriving cloud overlap statistics from radar. *Quarterly Journal of the Royal Meteorological Society*, *126*(569), 2903–2909. https://doi.org/10.1256/smsqj.56913

Jiang, J. H., Su, H., Zhai, C., Perun, V. S., Del Genio, A., Nazarenko, L. S., et al. (2012). Evaluation of cloud and water vapor simulations in CMIP5 climate models Using NASA "A-Train" satellite observations. *Journal of Geophysical Research Atmospheres*, *117*(14), n/a-n/a. https://doi.org/10.1029/2011JD017237

Kato, S., Rose, F. G., Sun-Mack, S., Miller, W. F., Chen, Y., Rutan, D. A., et al. (2011). Improvements of top-of-atmosphere and surface irradiance computations with CALIPSO-, CloudSat-, and MODIS-derived cloud and aerosol properties. *Journal of Geophysical Research Atmospheres*, *116*(19), 1–21. https://doi.org/10.1029/2011JD016050

Kay, J. E., & Gettelman, A. (2009). Cloud influence on and response to seasonal Arctic sea ice loss. *Journal of Geophysical Research Atmospheres*, *114*(18), 1–18. https://doi.org/10.1029/2009JD011773

Kay, J. E., L'Ecuyer, T., Chepfer, H., Loeb, N., Morrison, A., & Cesana, G. (2016). Recent Advances in Arctic Cloud and Climate Research. *Current Climate Change Reports*, *2*(4), 159–169. https://doi.org/10.1007/s40641-016-0051-9

Kiehl, J. T., & Trenberth, K. E. (1997). Earth's Annual Global Mean Energy Budget. *Bulletin of the American Meteorological Society*, *78*(2), 197–208. https://doi.org/10.1175/1520-0477(1997)078<0197:EAGMEB>2.0.CO;2

King, M. D., Platnick, S., Menzel, W. P., Ackerman, S. A., & Hubanks, P. A. (2013). Spatial and Temporal Distribution of Clouds Observed by MODIS Onboard the Terra and Aqua Satellites. *IEEE Transactions on Geoscience and Remote Sensing*, *51*(7), 3826–3852. https://doi.org/10.1109/TGRS.2012.2227333

Klein, S. A., & Hall, A. (2015). Emergent Constraints for Cloud Feedbacks. *Current Climate Change Reports*, *1*(4), 276–287. https://doi.org/10.1007/s40641-015-0027-1

Klein, S. A., McCoy, R. B., Morrison, H., Ackerman, A. S., Avramov, A., Boer, G. de, et al. (2009). Intercomparison of model simulations of mixed-phase clouds observed during the ARM Mixed-Phase Arctic Cloud Experiment. I: single-layer cloud. *Quarterly Journal of the Royal Meteorological Society*, *135*(641), 979–1002. https://doi.org/10.1002/qj.416

Klein, S. A., Zhang, Y., Zelinka, M. D., Pincus, R., Boyle, J., & Gleckler, P. J. (2013). Are climate model simulations of clouds improving? An evaluation using the ISCCP simulator. *Journal of Geophysical Research Atmospheres*, *118*(3), 1329–1342. https://doi.org/10.1002/jgrd.50141

Klein, S. A., Hall, A., Norris, J. R., & Pincus, R. (2017). Low-Cloud Feedbacks from Cloud-Controlling Factors: A Review. *Surveys in Geophysics*, *38*(6), 1307–1329. https://doi.org/10.1007/s10712-017-9433-3

Knobelspiesse, K., Barbosa, H. M. J., Bradley, C., Bruegge, C., Cairns, B., Chen, G., et al. (2020). The Aerosol Characterization from Polarimeter and Lidar (ACEPOL) airborne field campaign. *Earth System Science Data*, *12*(3), 2183–2208. https://doi.org/10.5194/essd-12-2183-2020

Komurcu, M., Storelvmo, T., Tan, I., Lohmann, U., Yun, Y., Penner, J. E., et al. (2014). Intercomparison of the cloud water phase among global climate models. *Journal of Geophysical Research: Atmospheres*, *119*(6), 3372–3400. https://doi.org/10.1002/2013JD021119

Kramer, R. J., Matus, A. V., Soden, B. J., & L'Ecuyer, T. S. (2019). Observation-Based Radiative Kernels From CloudSat/CALIPSO. *Journal of Geophysical Research: Atmospheres*, *124*(10), 5431–5444. https://doi.org/10.1029/2018JD029021

L'Ecuyer, T. S., Wood, N. B., Haladay, T., Stephens, G. L., & Stackhouse, P. W. (2009). Impact of clouds on atmospheric heating based on the R04 CloudSat fluxes and heating rates data set. *Journal of Geophysical Research Atmospheres*, *114*(8), 1–15. https://doi.org/10.1029/2008JD009951

L'Ecuyer, T. S., Beaudoing, H. K., Rodell, M., Olson, W., Lin, B., Kato, S., et al. (2015). The observed state of the energy budget in the early twenty-first century. *Journal of Climate*, *28*(21), 8319–8346. https://doi.org/10.1175/JCLI-D-14-00556.1

L'Ecuyer, T. S., Hang, Y., Matus, A. V., & Wang, Z. (2019). Reassessing the effect of cloud type on earth's energy balance in the age of active spaceborne observations. Part I: Top of atmosphere and surface. *Journal of Climate*, *32*(19), 6197–6217.

https://doi.org/10.1175/JCLI-D-18-0753.1
Li, J. L. F., Lee, W. L., Waliser, D., Wang, Y. H., Yu, J. Y., Jiang, X., et al. (2016). Considering the radiative effects of snow on tropical Pacific Ocean radiative heating profiles in contemporary GCMs using A-Train observations. *Journal of Geophysical Research*, *121*(4), 1621–1636. https://doi.org/10.1002/2015JD023587
Loeb, N. G., Wang, H., Allan, R. P., Andrews, T., Armour, K., Cole, J. N. S., et al. (2020). New Generation of Climate Models Track Recent Unprecedented Changes in Earth's Radiation Budget Observed by CERES. *Geophysical Research Letters*, *47*(5), 1–10. https://doi.org/10.1029/2019GL086705
Mace, G. G., & Wrenn, F. J. (2013). Evaluation of the hydrometeor layers in the East and West Pacific within ISCCP cloud-top pressure-optical depth bins using merged CloudSat and CALIPSO data. *Journal of Climate*, *26*(23), 9429–9444. https://doi.org/10.1175/JCLI-D-12-00207.1
Marchand, R., Ackerman, T., Smyth, M., & Rossow, W. B. (2010). A review of cloud top height and optical depth histograms from MISR, ISCCP, and MODIS. *Journal of Geophysical Research Atmospheres*, *115*(16), 1–25. https://doi.org/10.1029/2009JD013422
Matus, A. V., & L'Ecuyer, T. S. (2017). The role of cloud phase in Earth's radiation budget. *Journal of Geophysical Research*, *122*(5), 2559–2578. https://doi.org/10.1002/2016JD025951
McCoy, D. T., Eastman, R., Hartmann, D. L., & Wood, R. (2017). The change in low cloud cover in a warmed climate inferred from AIRS, MODIS, and ERA-interim. *Journal of Climate*, *30*(10), 3609–3620. https://doi.org/10.1175/JCLI-D-15-0734.1
McIlhattan, E. A., Kay, J. E., & L'Ecuyer, T. S. (2020). Arctic Clouds and Precipitation in the Community Earth System Model Version 2. *Journal of Geophysical Research: Atmospheres*, *125*(22). https://doi.org/10.1029/2020JD032521
Myers, T. A., & Norris, J. R. (2016). Reducing the uncertainty in subtropical cloud feedback. *Geophysical Research Letters*, *43*(5), 2144–2148. https://doi.org/10.1002/2015GL067416
Nam, C., Bony, S., Dufresne, J., & Chepfer, H. (2012). The ' too few , too bright ' tropical low-cloud problem in CMIP5 models, *39*(September), 1–7. https://doi.org/10.1029/2012GL053421
Narenpitak, P., & Bretherton, C. S. (2019). Understanding Negative Subtropical Shallow Cumulus Cloud Feedbacks in a Near-Global Aquaplanet Model Using Limited Area Cloud-Resolving Simulations. *Journal of Advances in Modeling Earth Systems*, 1600–1626. https://doi.org/10.1029/2018MS001572
Oreopoulos, L., Cho, N., Lee, D., Kato, S., & Huffman, G. J. (2014). An examination of the nature of global MODIS cloud regimes. *Journal of Geophysical Research: Atmospheres*, *119*(13), 8362–8383. https://doi.org/10.1002/2013JD021409
Pincus, R., Platnick, S., Ackerman, S. A., Hemler, R. S., & Hofmann, R. J. P. (2012). Reconciling Simulated and Observed Views of Clouds: $\lbrace$MODIS$\rbrace$, $\lbrace$ISCCP$\rbrace$, and the Limits of Instrument Simulators. *Journal of Climate*, *25*(13), 4699–4720. https://doi.org/10.1175/jcli-d-11-00267.1
Qu, X., Hall, A., Klein, S. A., & Caldwell, P. M. (2014). On the spread of changes in marine low cloud cover in climate model simulations of the 21st century. *Climate Dynamics*, *42*(9–10), 2603–2626. https://doi.org/10.1007/s00382-013-1945-z

Qu, X., Hall, A., Klein, S. A., & Deangelis, A. M. (2015). Positive tropical marine low-cloud cover feedback inferred from cloud-controlling factors. *Geophysical Research Letters*, *42*(18), 7767–7775. https://doi.org/10.1002/2015GL065627

Rossow, W. B., & Schiffer, R. A. (1999). Advances in Understanding Clouds from ISCCP. *Bulletin of the American Meteorological Society*, *80*(11), 2261–2287. https://doi.org/10.1175/1520-0477(1999)080<2261:AIUCFI>2.0.CO;2

Silber, I., Fridlind, A., Verlinde, J., Ackerman, A., Cesana, G., & Knopf, D. (2020). The Prevalence of Precipitation from Polar Supercooled Clouds. *Atmospheric Chemistry and Physics Discussions*, (October), 1–32. https://doi.org/10.5194/acp-2020-993

Soden, B. J., Held, I. M., Colman, R. C., Shell, K. M., Kiehl, J. T., & Shields, C. A. (2008). Quantifying climate feedbacks using radiative kernels. *Journal of Climate*, *21*(14), 3504–3520. https://doi.org/10.1175/2007JCLI2110.1

Stephens, G. L., Vane, D. G., Boain, R. J., Mace, G. G., Sassen, K., Wang, Z., et al. (2002). THE CLOUDSAT MISSION AND THE A-TRAIN. *Bulletin of the American Meteorological Society*, *83*(12), 1771–1790. https://doi.org/10.1175/BAMS-83-12-1771

Stephens, G. L., Li, J., Wild, M., Clayson, C. A., Loeb, N., Kato, S., et al. (2012). latest global observations. *Nature Geoscience*, *5*(10), 691–696. https://doi.org/10.1038/ngeo1580

Stubenrauch, C. J., Rossow, W. B., Kinne, S., Ackerman, S., Cesana, G., Chepfer, H., et al. (2013). Assessment of global cloud datasets from satellites. *Bulletin of the American Meteorological Society*, *94*(7), 1031–1049. https://doi.org/10.1175/BAMS-D-12-00117.1

Tan, I., Storelvmo, T., & Zelinka, M. D. (2016). Observational constraints on mixed-phase clouds imply higher climate sensitivity. *Science*, *352*(6282), 224–227. https://doi.org/10.1126/science.aad5300

Terai, C. R., Klein, S. A., & Zelinka, M. D. (2016). Constraining the low-cloud optical depth feedback at middle and high latitudes using satellite observations. *Journal of Geophysical Research*, *121*(16), 9696–9716. https://doi.org/10.1002/2016JD025233

Tselioudis, G., Rossow, W., Zhang, Y., & Konsta, D. (2013). Global weather states and their properties from passive and active satellite cloud retrievals. *Journal of Climate*, *26*(19), 7734–7746. https://doi.org/10.1175/JCLI-D-13-00024.1

Tsushima, Y., Emori, S., Ogura, T., Kimoto, M., Webb, M. J., Williams, K. D., et al. (2006). Importance of the mixed-phase cloud distribution in the control climate for assessing the response of clouds to carbon dioxide increase: A multi-model study. *Climate Dynamics*, *27*(2–3), 113–126. https://doi.org/10.1007/s00382-006-0127-7

Vial, J., Dufresne, J. L., & Bony, S. (2013). On the interpretation of inter-model spread in CMIP5 climate sensitivity estimates. *Climate Dynamics*, *41*(11–12), 3339–3362. https://doi.org/10.1007/s00382-013-1725-9

Wielicki, B. A., Barkstrom, B. R., Harrison, E. F., Lee, R. B., Louis Smith, G., & Cooper, J. E. (1996). Clouds and the Earth's Radiant Energy System (CERES): An Earth Observing System Experiment. *Bulletin of the American Meteorological Society*, *77*(5), 853–868. https://doi.org/10.1175/1520-0477(1996)077<0853:CATERE>2.0.CO;2

Winker, D. M., Pelon, J., Coakley, J. A., Ackerman, S. A., Charlson, R. J., Colarco, P. R., et al. (2010). The CALIPSO Mission. *Bulletin of the American Meteorological Society*, *91*(9), 1211–1230. https://doi.org/10.1175/2010BAMS3009.1

Zelinka, M. D., Zhou, C., & Klein, S. A. (2016). Insights from a refined decomposition of cloud

feedbacks. *Geophysical Research Letters*, *43*(17), 9259–9269. https://doi.org/10.1002/2016GL069917

Zelinka, M. D., Myers, T. A., McCoy, D. T., Po-Chedley, S., Caldwell, P. M., Ceppi, P., et al. (2020). Causes of Higher Climate Sensitivity in CMIP6 Models. *Geophysical Research Letters*, *47*(1), 1–12. https://doi.org/10.1029/2019GL085782

Zhang, M. H., Lin, W. Y., Klein, S. A., Bacmeister, J. T., Bony, S., Cederwall, R. T., et al. (2005). Comparing clouds and their seasonal variations in 10 atmospheric general circulation models with satellite measurements, *110*, 1–18. https://doi.org/10.1029/2004JD005021

Zhou, C., Zelinka, M. D., Dessler, A. E., & Klein, S. A. (2015). The relationship between interannual and long-term cloud feedbacks. *Geophysical Research Letters*, *42*(23), 10463–10469. https://doi.org/10.1002/2015GL066698